J Mol Model (2017) 23: 318
https://doi.org/10.1007/s00894-017-3488-4

ORIGINAL PAPER

Structures and stabilities of naturally occurring cyclodextrins: a theoretical study of symmetrical conformers

Juan José Gamboa-Carballo[1] · **Vijay Kumar Rana**[2] · **Joëlle Levalois-Grützmacher**[2] · **Sarra Gaspard**[3] · **Ulises Jáuregui-Haza**[1]

Received: 19 July 2017 / Accepted: 25 September 2017 / Published online: 20 October 2017

Abstract A molecular modeling study of symmetrical conformers of α-, β-, and γ-cyclodextrins in the gas and aqueous phases was carried out using the M06-2X density functional method, with SMD employed as an implicit solvation model. Eight symmetrical conformers were found for each cyclodextrin. Values of geometrical parameters obtained from the modeling study were found to agree well with those obtained from X-ray diffraction structures. A vibrational analysis using harmonic frequencies was performed to determine thermodynamic quantities. The GIAO method was applied to determine proton and carbon-13 NMR chemical shifts, which were then compared with corresponding chemical shifts reported in the literature. Hydrogen-bonding patterns were analyzed using geometrical descriptors, and quantum chemical topology was explored by QTAIM analysis. The results of this study indicated that four of the eight conformers studied for each cyclodextrin are the most populated in aqueous solution. These results provide the foundations for future studies of host–guest complexes involving these cyclodextrins.

Keywords Cyclodextrins · Density functional theory · Vibrational analysis · GIAO · QTAIM

Electronic supplementary material The online version of this article (https://doi.org/10.1007/s00894-017-3488-4) contains supplementary material, which is available to authorized users.

✉ Ulises Jáuregui-Haza
ulises.jauregui@infomed.sld.cu; ulises@instec.cu

[1] Instituto Superior de Tecnologías y Ciencias Aplicadas, Universidad de La Habana, Ave. Salvador Allende No. 1110, P.O. Box 6163, CP 10600 Plaza de la Revolución, La Habana, Cuba

[2] Department of Chemistry and Applied Biosciences, Laboratory of Inorganic Chemistry, ETH Zürich, Vladimir-Prelog-Weg 1-5/10, CH-8093 Zurich, Switzerland

[3] Laboratoire COVACHIM M2E, EA 3592 Université des Antilles, BP 250, 97157 Pointe-à-Pitrex CEDEX, Guadeloupe, French West Indies, France

Introduction

Cyclodextrins (CDs) are homochiral macrocyclic oligosaccharides formed by linking D-(+)glucopyranose subunits together via α-(1→4) glycosidic bonds [1]. CDs are obtained through the partial degradation of the amylose component of starch by the enzyme cyclodextrin glucosyltransferase [2, 3]. The structural formulae of the most common naturally occurring CDs (α, β, and γ; with six, seven, and eight glucopyranose units, respectively) can be found in several works [1, 4]. α, β, and γ are also the CDs that have received the most attention from researchers in the literature [4]. Figure 1 shows structural representations of these three CDs (both top and side views of each).

These carbohydrates are commonly described as being toroidal or shallow truncated conic in shape rather than cylindrical, due to the chair conformation of each glucopyranose building block. They have a hydrophilic exterior (shell), making them soluble in water; hydroxyl groups are present in both their outer and inner rims. Figure 2 shows a schematic of a single glucose unit from a CD.

In CDs, the inner rim contains primary hydroxyls (O6–H). The outer rim has secondary hydroxyls (O2–H and O3–H). CDs also have a cavity lined with hydrogen atoms and glycosidic oxygen bridges (O1), meaning that the cavity is weakly lipophilic (hydrophobic) [1] and can therefore capture hydrophobic molecules. This phenomenon is known as forming a molecular inclusion complex, also called a host–guest complex [8–11]. Various aspects of cyclodextrin chemistry have been discussed in several reviews [12–15].

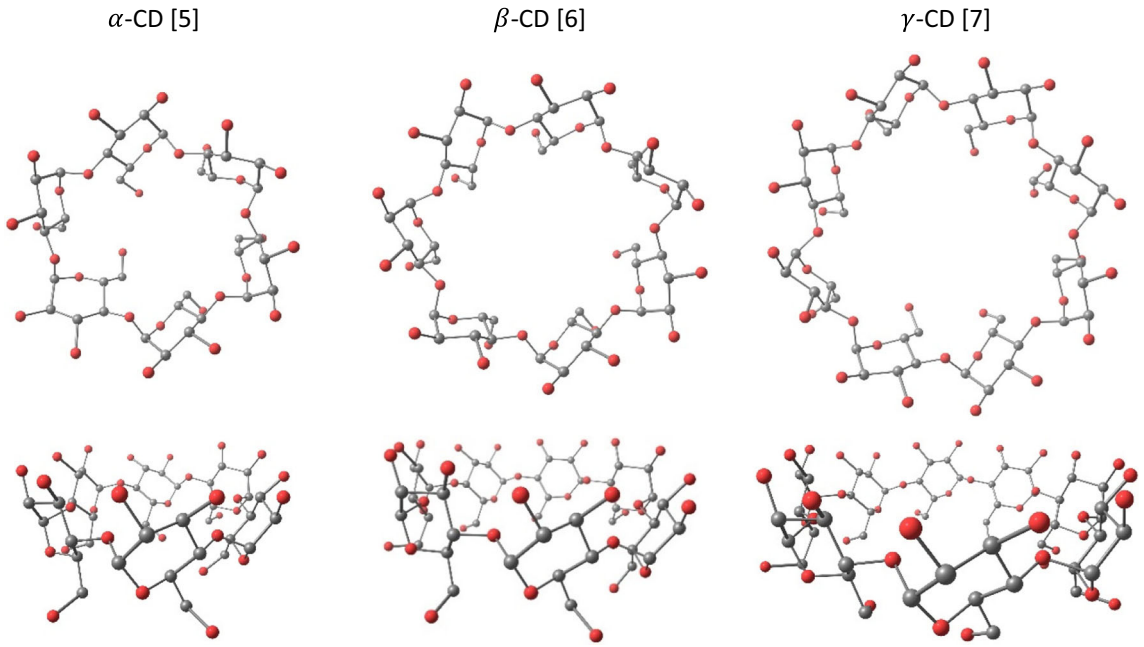

Fig. 1 Original X-ray diffraction structures of the CDs used in this work. Hydrogen atoms either did not appear in the original data or have been removed for clarity

CDs have been applied in many fields [4, 10, 16], including industry [17–19], pharmaceutical science [8, 20–23], environmental protection [24–26], food [27, 28], and analytical chemistry [29–32]. Applications of CDs usually make use of their ability to host guest molecules, and so the applications of a particular CD depend mainly on its diameter and the general conformation of its inner cavity [21].

Although CDs have a truncated cone structure, the glucopyranose units are very flexible as a consequence of the rotation and rapid proton exchange of the primary and secondary hydroxyl groups, and the C5–C6 bond shows a high degree of rotation. The glycosidic linkage is also able to rotate to some extent, meaning that each unit has a certain degree of mobility relative to the other units. This flexibility of the glucopyranose

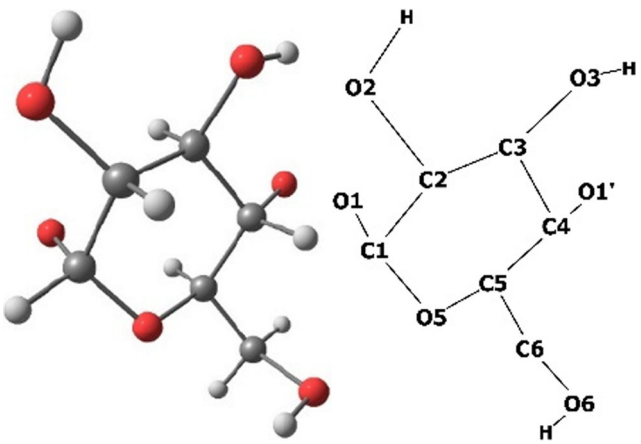

Fig. 2 Glucose unit from a CD, showing the atom labeling scheme applied

units of CDs makes it extremely difficult to describe a cyclodextrin using a single structure, as many conformers are possible for a particular CD at room temperature [33]. These conformers are expected to be in equilibrium in aqueous solution [33].

Several X-ray diffraction (XRD) structures have been determined for CDs and their derivatives [5–7, 34–36]. These structures vary in accordance with the conditions under which the crystals were synthesized and their level of hydration [6, 33], as varying these parameters can change the dominant conformer. The XRD structure observed in the solid phase may not be the most populated conformer in solution, meaning that XRD cannot unequivocally identify the structures and stabilities of CDs in solution [33]. Moreover, a complete conformational search of all possible conformers would lead to a huge amount of structures, even for the smallest CD, α.

Due to the size of these systems (CDs and host–guest complexes), the methods that have traditionally been used to determine their structures are molecular mechanics [37–40], semiempirical methods [41, 42], and low-level DFT and ab initio methods [42–44].

Several studies have reported the use of symmetrical conformers to describe the structures and stabilities of CDs and their derivatives in the gas phase and solution [40, 43–49]. In 1988, Koehler et al. [40] carried out a molecular dynamics study using the GROMOS force field to characterize the dynamical behavior of α-CD in aqueous solution. The mean geometry of α-CD over time was presented, and significant differences were reported between the conformation of this CD in aqueous solution

and that of α-CD in crystal form. Pinjari et al. presented a study that explicitly addressed the symmetrical conformers of α-, β-, and γ-CD [45]. They used the PM3 and B3LYP methods to investigate intramolecular hydrogen bonding and molecular electrostatic potential. A subsequent study in 2007 explored symmetrical conformers using Hartree–Fock (HF) theory and the B3LYP density functional method [46]. That work examined intramolecular hydrogen interactions by means of the GIAO chemical shifts of hydroxyl protons, and electron density topology using the quantum theory of atoms in molecules (QTAIM). Also in 2007, Karpfen et al. [47] studied symmetrical β-CD using the B3LYP and HF methods, forcing C_7 symmetry in all calculations. They found several stable hypothetical conformers and discussed cooperative hydrogen bonds. Moreover, Anconi et al. studied symmetrical α-CD conformers using HF and BLYP in the gas phase and in aqueous solution (applying the PCM model as an implicit solvation scheme). In that work, they identified the most favorable structures in the gas phase and aqueous solution by studying thermodynamic quantities. In the same year, Snor et al. reported a study of anhydrous β-CD using the B3LYP method in which C_7 symmetry was imposed. In 2008, Jiménez et al. [48] presented a study of α-CD using HF, B3LYP, and X3LYP, in which geometry optimization was performed and the effects of PCM solvation were examined. More recently, Deshmukh et al. studied the cooperative hydrogen interactions in α-, β-, and γ-CD conformers using B3LYP and by imposing C_n symmetry during optimization, where *n* is the number of glucose units [49]. Also in 2011, Stachowicz et al. [50] reported a study of the interactions of symmetrical conformers of β-CD with positive metal ions. A very recent study by Jaiyong et al. [51] depicted the interactions of symmetrical β-CD conformers using several methods, including density functionals with high-quality basis sets and other approximate quantum-chemical methods. They also used conformers that were previously studied by Snor et al. [44] and Stachowicz et al. [50] in order to compare values and trends. Those studies focused on specific characteristics or phenomena of CDs. However, there has not been an exhaustive study of all three CDs using state-of-the-art methodologies in the last few years.

In the last decade, modern computational methods such as the Minnesota series of density functionals [52] have gained prominence in the literature. Moreover, recent advances in high-performance computing and hardware setups make it possible to use more accurate methods to describe relatively large systems such as CDs. Thus, the aim of the work reported in the present paper was to update the data available from theoretical calculations of CDs using up-to-date methodologies, in order to lay the foundations for further studies on molecular inclusion complexes involving CDs.

Methods

System under study

The system under study consisted of symmetrical conformers built from the XRD structures of α-CD [5], β-CD [6], and γ-CD [7] (Fig. 1).

The conformers were generated by rotating the "free" bonds of the glucopyranose units: C2–O2 and C3–O3 for secondary hydroxyls, and C5–C6 and C6–O6 for primary hydroxyls (Fig. 2). Each dihedral was rotated by 10° while enforcing C_n symmetry, where *n* is the number of glucopyranose units. The geometries obtained were first optimized using the semiempirical Hamiltonian PM6-D3H4 [53–55] as implemented in the MOPAC2016 calculation package [56]. As a result of the conformational search and optimization, all of the structures collapsed into a set of 24 stable symmetrical conformers (eight for each CD). These conformers differed from each other in the hydrogen interaction patterns of their inner and outer rims. Figure 3 shows the eight conformers for α-CD.

The obtained conformers were classified into three groups: A, B, and C, as also done by other authors in the literature [46, 49]. Conformers type A are characterized by O6–H···O6′ hydrogen interactions with the primary hydroxyls oriented to the cavity, forming a ring of hydrogen bonds between adjacent primary hydroxyls; B type conformers have O6–H···O5′ hydrogen interactions, and C type conformers have the primary hydroxyls pointing to the exterior of the CD with possible hydrogen interactions with the O5 of the same glucopyranose unit (O6–H···O5).

The conformers were also categorized according to the orientation of the hydrogen interaction pattern. Viewing from the top of the secondary (i.e., outer) rim, type 1 conformers present counterclockwise and clockwise orientations of their secondary and primary hydroxyls, respectively, while type 2 conformers exhibit the opposite orientation. Type 3 conformers present counterclockwise orientations of both their secondary and primary hydroxyls,whereas type 4 conformers show clockwise patterns for both secondary and primary hydroxyls. The reader is advised to be careful when comparing the geometries obtained here with those reported in the literature, as some differences may be observed, mainly regarding dihedral angles.

Computational details

In order to describe the geometries and wavefunctions of the obtained structures in an accurate way, the DFT hybrid functional M06-2X [52] and with Pople's split valence double-ζ basis set 6-31G(d,p) were applied to all conformers. DFT-D3 corrections [54] were also implemented with zero damping [57]. To deal with solvation effects, the SMD method [58]

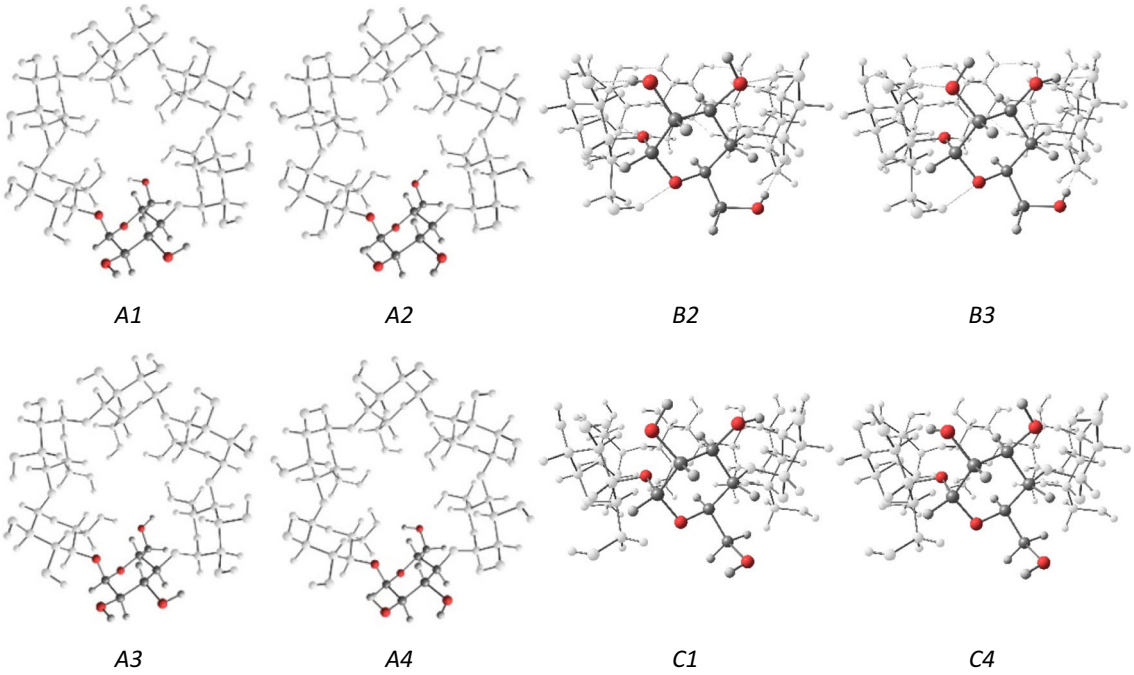

Fig. 3 Symmetrical conformers of α-CD, generated using PM6-D3H4. One glucose unit is detailed in each conformer to aid clarity

was used as an implicit solvation model (SMD/M06-2X/6-31G(d,p)). In almost every DFT calculation we performed, water was used as the solvent, except for the ^{1}H NMR studies, where dimethylsulfoxide (DMSO) was used. All DFT calculations were performed using the Gaussian09 package [59]. For all quantum calculations performed using the four methods described above, full eigenvector following geometry optimizations were carried out without any symmetry constraints.

In order to validate the methods used, the experimental XRD structures and the optimized conformers were compared in terms of bond distances and bond angles. The criterion used to compare these structures was the root mean square deviation (RMSD), as presented below:

$$RMSD = \sqrt{\frac{1}{N}\sum_{i=1}^{N}\left(\frac{X_{\text{theo},i}-X_{\text{XRD},i}}{X_{\text{XRD},i}}\right)^2} \times 100\%. \quad (1)$$

In Eq. 1, N represents the number of determined values and X_{theo} is the value of the parameter (bond length or bond angle) as calculated by the computational method. X_{XRD} is the value of the same parameter as assessed experimentally using XRD.

For DFT calculations, frequencies were calculated to prove the existence of a real minimum for each conformer. Thermodynamic parameters were extracted from the results of gas-phase (M06-2X/6-31G(d,p)) and aqueous (SMD/M06-2X/6-31G(d,p)) Gaussian09 calculations in order to evaluate the solvation process based on the total energy of electrons plus nuclear repulsion (ΔE), enthalpy (ΔH_{aq}), and free energy (ΔG_{aq}) for calculations in aqueous solution, as well as the variation in the free energy during the solvation process ($\delta\Delta G$) as presented in the following equation:

$$\delta\Delta G = \Delta G_{\text{aq}} - \Delta G_{\text{gas}}. \quad (2)$$

Here, the subscripts "gas" and "aq" refer to calculations performed with the CDs in the gas phase and in aqueous solution, respectively.

ΔH_{aq} and ΔG_{aq} values were reported with respect to a selected reference value according to the following equation:

$$\Delta Y = \Delta Y_i - \Delta Y_{\text{ref}}, \quad (3)$$

where ΔY_i is the value of the parameter (i.e., ΔH or ΔG) calculated for a given conformer and ΔY_{ref} is a reference value for the same parameter (in this work, the reference value is the value obtained for one of the calculated conformers). This approach allows the reader to compare the results in a more comfortable way.

With the same aim, a new parameter was constructed from ΔE. The parameter $\Delta E/n$ is the total energy divided by the number of glucopyranose units. The results are presented using the appropriate minimum value (the values for the A3 conformer of α-CD in the gas phase and the B2 conformer of γ-CD in aqueous solution) as a reference in accordance with the equation

$$\Delta E/n = \frac{\Delta E_i}{n_i} - \frac{\Delta E_{\text{ref}}}{n_{\text{ref}}}, \quad (4)$$

where the subscript i refers to the conformer of interest and "ref" indicates the reference conformer. This new parameter

allowed us to compare CDs in terms of ΔE even when the CDs were different sizes. Also, from hereon, we use the term "total energy" to refer to the "total energy of electrons plus nuclear repulsion" for the sake of brevity.

Dipole moments were calculated at the SMD/M06-2X/6-31G(d,p) level of theory using water as an implicit solvent, as many computational studies have predicted high dipole moments along the *z*-axis for all three CDs [33].

Geometries and wavefunctions obtained via M06-2X were employed to calculate proton and ^{13}C NMR spectra using the gauge including atomic orbitals (GIAO) method [60, 61], which has proven to be an adequate approximation for correlating theoretical chemical shifts with experimental NMR spectra [62, 63]. Chemical shifts are reported in ppm using the IUPAC convention. In all cases, tetramethylsilane (TMS) was used as a reference with a chemical shift of 0.0 ppm. The solvent used when calculating the theoretical ^{1}H NMR spectra was dimethylsulfoxide (DMSO), in order to simulate experimental DMSO-d_6 solvation effects. For the calculations of ^{13}C spectra, water was used as an implicit solvent to simulate a deuterium oxide (D_2O) environment.

Using the DFT results for the CDs in aqueous solution, further analysis of possible hydrogen interactions was then carried out. The first set of criteria used to compare hydrogen interactions were geometrical, i.e., interaction distances and angles, as several studies have reported correlations between these parameters and the strength and stability of the interactions [64–67]. However, these are not the definitive parameters for classifying interactions [67].

A second set of criteria were employed when exploring quantum chemical topology using the quantum theory of atoms in molecules (QTAIM) pioneered by Bader [68]. The first criterion to be established was the presence of a bond critical point (BCP) and a bond path between the interacting atoms. Further description and classification of these interactions was achieved using several descriptors of the electron density at the BCP, such as the electron density (ρ_c), the Laplacian of the electron density ($\nabla^2\rho_c$), the total energy density (H_c), and the ellipticity of the electron density (ε_c). The obtained parameters were used to classify the hydrogen interactions according to Nakanishi's classification criteria [69, 70].

Results and discussion

Validating the geometries

A comparison of the geometries of the conformers obtained in this work with their corresponding XRD structures is shown in Fig. 4. This graphic shows the agreement of the XRD experimental bond lengths and angles with the corresponding quantities obtained using the SMD/M06-2X/6-31G(d,p) methodology. The results shown in the figure are averages across the eight conformers for each of α-, β-, and γ-CD, respectively.

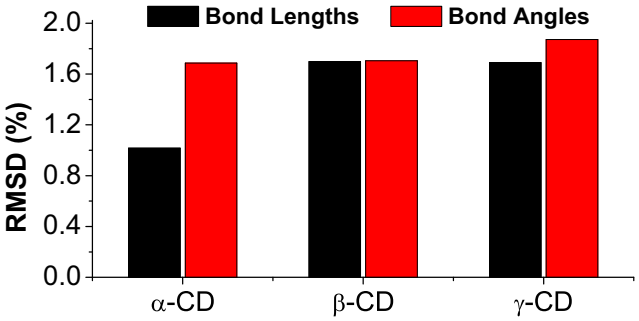

Fig. 4 Root mean square deviations (RMSDs) in bond lengths and angles between X-ray diffraction geometries and the geometries obtained using the SMD/M06-2X/6-31G(d,p) methodology. Water was used as solvent in the SMD implicit solvation scheme

From Fig. 4, it is clear that the SMD/M06-2X/6-31G(d,p) methodology gives adequate results when compared to the XRD geometries, as the RMSDs in bond lengths and angles are always less than 2%. Comparisons of all the conformers regarding their geometrical parameters are presented in Tables S1–S6 and Fig. S1–S6 of the "Electronic supplementary material" (ESM). We could not detect any significant differences in the RMSDs in bond lengths and angles when comparing the conformers. For this reason, these geometrical parameters (bond lengths and bond angles) could not be used in this work to select the most probable conformers in aqueous solution. This result indicates that comparisons of solid-state structures with modeled gas-phase or solvated structures may not be adequate [33].

Thermodynamics

For DFT calculations, an analysis of some thermodynamic parameters of the conformers was performed, comparing the results calculated with and without implicit solvation. Figure 5 shows the results attained using the scheme M06-2X/6-31G(d,p) for the parameter $\Delta E/n$, while Fig. 6 shows the results obtained using SMD with water as an implicit solvent.

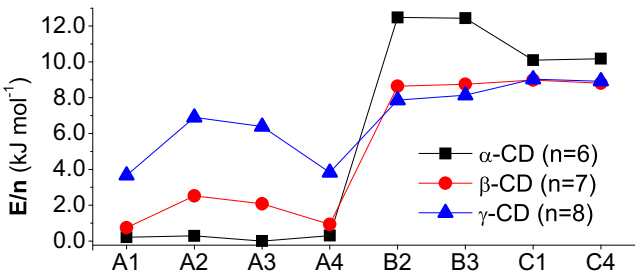

Fig. 5 Total energy of electrons plus nuclear repulsions per glucose unit ($\Delta E/n$) of each optimized CD in the gas phase, calculated at the M06-2X/6-31G(d,p) level of theory. All values are presented relative to the minimum value (obtained for the A3 conformer of α-CD)

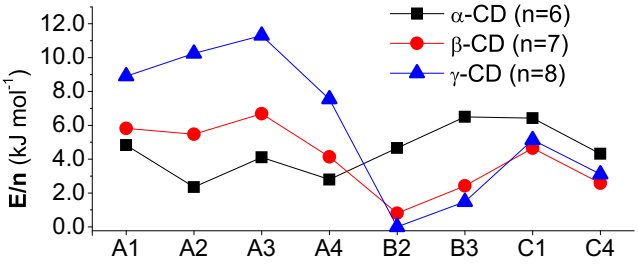

Fig. 6 Total energy of electrons plus nuclear repulsions per glucose unit ($\Delta E/n$) of each optimized CD in aqueous solution, as calculated at the SMD/M06-2X/6-31G(d,p) level of theory. All values are presented relative to the minimum value (obtained for the B2 conformer of γ-CD)

As can be observed from Fig. 5, the lowest energy (i.e., indicating the greatest stability) in the gas phase was obtained for conformer A3 of α-CD. In general, type A conformers are more stable than type B and C conformers, with a difference of over 12 kJ mol^{-1} per glucopyranose unit observed between the A3 and B2 conformers of α-CD. On the other hand, when using the SMD scheme (Figure 6), the behavior of this parameter shifts, especially for β- and γ-CD, for which the B and C conformers are more stable in aqueous solution. For α-CD, the difference observed in Fig. 6 is smaller than that seen in Fig. 5. This analysis suggests that B and C conformers may be more stable in aqueous solution than A conformers, and thus that B and C are the main conformers in aqueous solution. However, the results indicate that type A conformers are more likely to be observed in the gas phase than type B and C conformers, an inference supported by calculations in other works [46, 47]. However, the total energy may not be the best criterion for predicting this behavior.

Table 1 shows a comparison of the values of other thermodynamic parameters that can be used to decide whether a conformer is stable in aqueous solution. The absolute values obtained in all thermodynamic calculations are reported in Tables S7 and S8 of the ESM.

The values for all of the parameters presented in Table 1 indicate that the B and C conformers are the most stable, especially in β- and γ-CD, where solvation effects should be more pronounced due to an increase in the number of the hydroxyl groups in the molecule with respect to α-CD. Moreover, values of the parameter $\delta\Delta G$, which dictates whether the solvation process is spontaneous, indicate that the stabilities of B and C conformers are higher in solution than in the gas phase. These results agree with those obtained by Anconi et al. for α-CD using the BLYP hybrid DFT functional [43]; they observed similar solvation behavior for their type 2 and 3 conformers, which were similar to the type B and C conformers in this work. On the other hand, the high values of $\delta\Delta G$ for the B and C conformers of β-CD contradict the experimental results, as β-CD is the least water soluble of all the natural CDs [21]. This constitutes a limitation of our model, as it cannot explain this experimental behavior, which has been the subject of several debates [33]. Moreover, no corrections were made to frequencies used to calculate the free energy at room temperature, so these data should only be compared with other values obtained in this work. However, this result is important in the context of selecting a set of structures that could be used as building blocks for future research into molecular inclusion complexes of CDs.

For the reasons given above, the implicit solvation formalism SMD is very useful for describing the thermodynamics and the order of stability of the studied conformers. It can also provide insight into the average conformations of these CDs in aqueous solution. Such results indicate the conformers that should be used when conducting computational studies of host–guest complexes.

Table 1 Calculated values of the relative total energy of electrons plus nuclear repulsion (ΔE), the aqueous enthalpy (ΔH_{aq}), the free energy (ΔG_{aq}), and the solvation free energy ($\delta\Delta G$) for the conformers in aqueous solution; calculations were performed at the M06-2X/6-31G(d,p) level of theory with water included as an implicit solvent using SMD

Parameter	CD	Conformer							
		A1	A2	A3	A4	B2	B3	C1	C4
ΔE	α-CD	0.0	−14.9	−4.3	−12.2	−1.0	10.0	9.6	−3.1
	β-CD	0.0	−2.4	6.1	−11.7	−35.1	−23.8	−8.1	−22.7
	γ-CD	0.0	10.7	19.2	−10.9	−71.3	−59.4	−30.1	−46.4
ΔH_{aq}	α-CD	0.0	−18.7	−11.9	−15.9	1.2	11.3	11.0	−0.3
	β-CD	0.0	−5.4	3.7	−10.9	−30.7	−19.8	−9.5	−23.1
	γ-CD	0.0	8.9	12.6	−8.9	−68.8	−56.9	−36.4	−50.5
ΔG_{aq}	α-CD	0.0	−19.1	−19.4	−19.9	−5.8	−0.5	−10.6	−20.2
	β-CD	0.0	−9.8	10.1	−9.6	−33.7	−23.9	−41.6	−52.9
	γ-CD	0.0	6.7	10.0	−3.5	−64.1	−52.4	−57.0	−68.0
$\delta\Delta G$	α-CD	0.0	−20.2	−16.9	−21.9	−73.3	−66.1	−45.3	−56.5
	β-CD	0.0	−22.0	2.1	−13.0	−92.6	−75.8	−78.6	−87.2
	γ-CD	0.0	−7.2	−5.0	−1.8	−86.1	−70.9	−69.2	−77.4

All values are given in kJ mol^{-1} relative to the value obtained for conformer A1

Dipole moments

The dipole moments of CDs have also been investigated in other works. Several studies have suggested high dipole moments for the CDs presented in this work [12, 33]. The complementarity of the dipoles between CDs and guest molecules has also been discussed [71]. Table 2 displays the dipole moments for all 24 conformers treated in the present work.

Given that the structures studied here have symmetries close to C_n, only the *z*-components of the dipole moments are displayed in Table 2; the other components are neglected. Twenty-three of the 24 structures have their dipoles oriented toward the secondary hydroxyls, with only conformer A1 of γ-CD having the opposite orientation. The highest dipoles were calculated for the B2 and B3 conformers of β- and γ-CD. The obtained results do not permit us to draw conclusions about the main conformations of the CDs in aqueous solution, even if we assume that CDs have high dipole moments, which is an assumption based only on theoretical calculations, not experiment [71–73]. Moreover, the A2 and A3 conformers have particularly high dipole moments, and the C-type conformers have very low ones when compared with B2 and B3, which makes us question the use of this parameter to select the conformers that best describe the CDs in solution. According to Pinjari et al. [46], their conformers of type A, which are almost identical to the A-type conformers proposed in this work, present low dipole moments when compared with the B and C types. That work also reported two negative values for the A4 conformers of β-CD and γ-CD, whereas only one negative value was detected (for the A1 conformer of γ-CD) in the present work. It should be noted that Pinjari et al. [46] calculated the dipole moments at the B3LYP/6-31G(d,p) level of theory. Additionally, there are some geometrical differences between the B- and C-type conformers in that work and those in the present work, meaning that not all of the conformers can be compared between works.

NMR studies

NMR spectroscopy is a very useful technique for determining chemical information. The obtained spectra are very sensitive to the geometrical structures and electron densities of the molecules studied. However, this sensitivity of NMR also has drawbacks in computational chemistry, as simulated NMR results are very sensitive to the particular method and basis set applied [61]. DFT hybrid functionals have been shown to yield good results for medium to large basis sets, with 6-31G(d,p) being close to the smallest basis set that can provide accurate results [61].

Typically, NMR is a "slow" spectroscopic technique when compared to the timescale for conformational changes of CDs at room temperature [74]. It should also be noted that magnetic pulses are applied to an enormous number of molecules, which means that NMR measurements are averaged over time and space. These limitations imply that signals from atoms located at the same position on different glucopyranose units are not distinguished in a NMR spectrum. For this reason, NMR spectra will always lead to symmetrical CDs, which makes this technique very interesting and useful for comparing experimental NMR spectra with the theoretical results obtained by GIAO.

Tables 3 and 4 show comparisons between theoretical (GIAO) and experimental results [36, 74] for the ^{1}H and ^{13}C chemical shifts, respectively, associated with the CDs studied in the present work.

All chemical shifts were calculated using TMS as reference and are reported in parts per million (ppm). The results of theoretical NMR calculations are reported relative to experimental chemical shifts. All absolute shift values for ^{1}H and ^{13}C NMR spectra (Tables S9 and S10), along with correlation graphics for the ^{1}H NMR data (Fig. S7) are presented in the ESM. According to the RMSD values and the correlation coefficients (*R*) between the theoretical and experimental NMR data, the theoretical results for the type B and C conformers are consistent with the corresponding experimentally determined proton and ^{13}C chemical shifts.

Regarding the ^{1}H NMR spectra, the theoretical results for the type B and C conformers correlate better with the corresponding experimental results based on the *R* values—especially B3 and C1, for which the *R* values are over 0.98. This indicates that linear scaling of the obtained chemical shifts may improve the theoretical NMR results and reduce RMSDs, as has been already reported [62, 63, 75]. However, the signal corresponding to the anomeric hydrogen (H1) is located at a significantly higher value of δ when compared with the other proton signals, which are grouped together. This behavior could lead to mistaken judgments about how well the experimental and theoretical data agree, due to the statistical limitations of the correlation analyses. For this reason, we also examined the RMSDs, which were lower for the B- and C-type conformers, in agreement with the correlation coefficients (*R*). Pinjari et al. [46] reported a GIAO study that used B3LYP to calculate proton chemical shifts. They reported linear correlations of the chemical shifts of active (O–H)

Table 2 Dipole moments along the *z*-axis (in debyes), as calculated at the SMD/M06-2X/6-31G(d,p) level of theory

CD	Conformer							
	A1	A2	A3	A4	B2	B3	C1	C4
α-CD	2.33	4.91	4.90	2.65	4.74	4.84	1.28	1.16
β-CD	1.20	4.97	4.61	1.62	7.14	6.92	0.79	0.95
γ-CD	−1.27	4.93	3.68	0.03	9.89	9.22	0.93	1.58

Dipole moments were calculated from the primary to the secondary rim. A negative value indicates an inversion of the dipole direction

Table 3 Values of proton chemical shifts for the CDs of interest, as calculated at the SMD/M06-2X-D3/6-31G(d,p) level of theory with DMSO as the solvent using GIAO

Signal	δ^a (ppm)	$\Delta\delta^b$ (ppm)							
		A1	A2	A3	A4	B2	B3	C1	C4
α-CD									
H1	4.79	0.05	−0.11	0.00	−0.06	0.22	0.33	0.25	0.13
H2	3.29	0.16	−0.12	0.18	−0.13	−0.04	0.26	0.14	−0.15
H3	3.78	0.09	0.05	0.09	0.05	−0.05	0.03	0.15	0.09
H4	3.40	−0.44	−0.27	−0.45	−0.26	0.37	0.17	0.10	0.29
H5	3.59	0.51	0.51	0.53	0.50	0.33	0.38	0.09	0.05
H6a,b	3.65	0.57	0.63	0.59	0.61	0.16	0.15	0.28	0.29
RMSD		0.37	0.36	0.38	0.34	0.23	0.25	0.18	0.19
R		0.83	0.81	0.80	0.83	0.95	0.98	0.99	0.96
β-CD									
H1	4.82	0.09	−0.10	0.03	−0.03	−0.15	0.22	0.24	0.12
H2	3.29	0.17	−0.12	0.18	−0.13	−0.05	0.27	0.12	−0.20
H3	3.64	0.12	0.07	0.09	0.11	0.10	0.11	0.15	0.14
H4	3.34	−0.39	−0.24	−0.43	−0.21	0.34	0.16	0.13	0.30
H5	3.59	0.49	0.46	0.47	0.49	0.25	0.27	0.08	0.07
H6a,b	3.64	0.63	0.68	0.64	0.67	0.02	0.16	0.33	0.36
RMSD		0.37	0.36	0.38	0.36	0.19	0.21	0.19	0.22
R		0.85	0.82	0.83	0.84	0.95	0.99	0.99	0.95
γ-CD									
H1	4.89	0.05	−0.15	−0.03	−0.06	0.09	0.19	0.18	0.03
H2	3.32	0.12	−0.18	0.12	−0.17	−0.12	0.17	0.04	−0.23
H3	3.65	0.06	0.06	0.04	0.10	0.03	0.03	0.34	0.12
H4	3.36	−0.40	−0.25	−0.46	−0.23	0.32	0.13	0.04	0.28
H5	3.56	0.56	0.59	0.57	0.52	0.21	0.22	0.29	0.02
H6a,b	3.65	0.63	0.69	0.64	0.66	0.07	0.06	0.31	0.23
RMSD		0.39	0.40	0.40	0.37	0.17	0.15	0.24	0.18
R		0.84	0.79	0.81	0.83	0.97	0.99	0.98	0.95

All values were calculated using TMS as reference. *RMSD* is the root mean square deviation of the theoretical value from the experimental value, and *R* is the correlation coefficient. The numbering scheme for the hydrogen atoms reflects the number labels of the carbons they are attached to (see Fig. 2).

[a] Experimental proton shifts [74]. [b] Values are reported relative to experimental shifts

protons with geometry- or electron-density-related parameters. Those results support the validity of the GIAO results obtained in this work, although only C–H protons were analyzed in the present work. Another critical marker is the average signal from CH_2 protons (H6a,b), which is in better agreement with the experimental results for B and C conformers than for A conformers. It was found in previous experimental NMR studies that these methylene hydrogen atoms, which have near-isochronous shifts, are likely to be both positioned gauche with respect to H5 for CDs in solution [74], as they are in the B and C conformers.

Correlation analysis of the ^{13}C spectra gives little information, since the *R* values are >0.99 for all conformers of the three CDs. However, the RMSD values corroborate the results from proton analysis, as smaller values were obtained for the B and C conformers.

The calculated NMR data are in good agreement with thermodynamic data obtained at the SMD/M06-2X/6-31G(d,p) level of theory.

Although experimental and theoretical proton shifts were obtained using DMSO as the solvent, this solvent is also able to form hydrogen bonds with CDs, meaning that CDs in DMSO show similar conformational behavior to CDs in aqueous solution. Thus, these results again point to a prevalence of B and C conformers of CDs in water.

Hydrogen interactions

Based on the XRD crystal structures of the CDs, it can be stated that intramolecular O–H···O interactions favor macrocyclic CD conformations, and may even govern the interactions of the CDs with molecules in their cavities (guests) [13,

Table 4 Values of ^{13}C chemical shifts for the CDs of interest, as calculated at the SMD/M06-2X-D3/6-31G(d,p) level of theory with H_2O as the solvent using GIAO

Signal	δ^a ppm)	$\Delta\delta^b$ (ppm)							
		A1	A2	A3	A4	B2	B3	C1	C4
α-CD									
C1	102.19	1.94	2.11	1.33	2.74	2.87	2.00	2.10	3.18
C2	72.61	2.89	3.20	2.71	3.50	3.76	3.02	3.60	3.91
C3	74.21	3.50	4.91	3.98	4.35	4.19	3.31	2.00	3.58
C4	82.07	5.83	2.81	4.76	3.95	−0.04	1.74	2.22	0.30
C5	72.91	5.39	7.53	6.84	6.05	4.55	3.79	2.21	2.82
C6	61.37	5.08	2.86	2.85	5.04	2.61	2.56	1.68	1.80
RMSD		4.34	4.31	4.13	4.40	3.35	2.83	2.38	2.87
R		0.99	0.99	0.99	1.00	0.99	1.00	1.00	1.00
β-CD									
C1	102.58	2.41	2.71	1.95	3.32	3.67	2.73	2.71	3.75
C2	72.67	3.85	3.82	3.36	4.10	4.30	3.87	4.42	4.64
C3	73.89	3.63	4.88	3.92	4.40	3.93	3.17	2.16	3.52
C4	81.94	6.31	3.93	5.83	4.55	1.45	3.11	2.83	1.21
C5	72.89	5.53	7.75	7.02	6.27	4.93	4.17	2.79	3.35
C6	61.17	5.12	3.21	3.21	5.20	2.75	2.68	2.56	2.64
RMSD		4.66	4.68	4.55	4.73	3.68	3.33	3.00	3.36
R		1.00	0.99	0.99	1.00	1.00	1.00	1.00	1.00
γ-CD									
C1	102.42	3.59	3.93	2.89	4.42	4.96	3.99	2.66	4.13
C2	73.19	3.25	4.05	3.39	3.93	4.68	4.21	3.59	3.97
C3	73.82	3.63	4.68	4.04	4.17	3.56	2.77	1.91	2.80
C4	81.33	8.74	5.77	7.63	6.79	3.36	5.08	2.69	1.50
C5	72.69	5.76	8.17	7.28	6.73	5.62	4.71	3.04	3.77
C6	61.21	6.18	3.60	3.70	6.04	1.99	2.08	2.43	2.29
RMSD		5.54	5.27	5.18	5.48	4.20	3.95	2.77	3.22
R		0.99	0.99	0.99	1.00	1.00	1.00	1.00	1.00

All values were calculated using TMS as reference. *RMSD* is the root mean square deviation of the theoretical value from the experimental value, and *R* is the correlation coefficient.

[a] Experimental ^{13}C shifts [36]. [b] Values are reported relative to experimental shifts

76]. Therefore, studying the hydrogen interactions in CDs is a crucial step when attempting to accurately describe the structures and properties of the CDs.

Table 5 shows the hydrogen-bond distances along with their standard deviations (in parentheses) for the studied cyclodextrins. Table 6 presents similar information regarding their hydrogen interaction angles. It has been stated that these parameters are often correlated with other electron-density-based, thermodynamic, and spectroscopic parameters [64–67]. It has also been stated that, for the same type of interaction, the smaller the distance, the greater the strength. Also, due to the directional character of these interactions, O–H···O angles of close to 180° are favored.

From Table 5, it can be seen that the smallest distances are obtained for the O6–H···O6′ interactions of type A conformers; these also have angles of close to 180° (Table 6). These interactions are likely to be the strongest of all those considered, as also reported by Deshmukh et al. [49] and Pinjari et al. [46], contributing some extra rigidity to the CDs and almost closing the primary face, which may hinder possible complex formation with a guest molecule both thermodynamically and kinetically. Also, the planar configuration of the chain of hydrogen bonds prevents strong interactions of surrounding water molecules with the primary hydroxyls. For the secondary hydroxyls, the studied interactions are most favorable for the C1 and C4 conformers, as they have the smallest interaction distances for O3–H···O2′ and O2–H···O3, respectively. These interactions are very important for maintaining the CDs in a bucket-like conformation while retaining sufficient flexibility to accommodate an incoming guest and to interact with the solvent. For B-type conformers, the interaction distances for O6–H···O5′ are similar to those of secondary hydroxyls, but the nature (i.e., hydroxyl–ether) of

Table 5 Values of the mean hydrogen interaction distance and the standard deviations in these values (all in Å) for the CDs, as calculated at the SMD/M06-2X-D3/6-31G(d,p) level of theory

Interaction	A1		A2		A3		A4		B2		B3		C1		C4	
α-CD																
O3–H···O2′	2.16	(0.13)			2.10	(0.00)					2.12	(0.01)	1.97	(0.01)		
O2–H···O3′			2.15	(0.01)			2.20	(0.15)	2.17	(0.01)					2.03	(0.00)
O6–H···O6′	1.81	(0.01)	1.84	(0.00)	1.84	(0.00)	1.82	(0.01)								
O6–H···O5′									2.05	(0.02)	2.03	(0.02)				
O6–H···O5													2.43	(0.02)	2.45	(0.02)
β-CD																
O3–H···O2′	2.08	(0.07)			2.06	(0.01)					2.05	(0.01)	1.96	(0.01)		
O2–H···O3′			2.11	(0.02)			2.14	(0.11)	2.09	(0.01)					2.00	(0.01)
O6–H···O6′	1.85	(0.03)	1.89	(0.01)	1.87	(0.01)	1.87	(0.02)								
O6–H···O5′									2.02	(0.02)	2.01	(0.02)				
O6–H···O5													2.52	(0.04)	2.55	(0.02)
γ-CD																
O3–H···O2′	2.05	(0.02)			2.05	(0.03)					2.02	(0.00)	1.95	(0.02)		
O2–H···O3′			2.10	(0.02)			2.10	(0.06)	2.07	(0.00)					1.99	(0.05)
O6–H···O6′	1.94	(0.01)	1.96	(0.03)	1.93	(0.05)	1.96	(0.01)								
O6–H···O5′									1.99	(0.01)	1.98	(0.02)				
O6–H···O5													2.51	(0.07)	2.50	(0.06)

Table 6 Values of the mean hydrogen interaction angle and the standard deviations in these values (all in degrees) for the CDs, as calculated at the SMD/M06-2X-D3/6-31G(d,p) level of theory

Interaction	A1		A2		A3		A4		B2		B3		C1		C4	
α-CD																
O3–H···O2′	163.7	(3.8)			163.9	(0.5)					163.4	(0.3)	163.3	(0.7)		
O2–H···O3′			153.4	(0.0)			152.9	(3.0)	153.7	(0.5)					155.0	(0.4)
O6–H···O6′	169.2	(5.8)	168.2	(0.2)	168.1	(0.4)	168.7	(6.1)								
O6–H···O5′									146.1	(1.4)	148.3	(1.4)				
O6–H···O5													104.5	(0.6)	104.1	(0.8)
β-CD																
O3–H···O2′	162.1	(3.2)			161.9	(0.4)					161.7	(0.5)	160.9	(1.0)		
O2–H···O3′			151.6	(0.8)			150.8	(2.6)	152.2	(0.6)					153.0	(0.6)
O6–H···O6′	169.1	(5.6)	164.6	(1.2)	164.7	(0.7)	168.2	(3.7)								
O6–H···O5′									147.8	(1.2)	149.9	(1.2)				
O6–H···O5													102.8	(0.8)	102.4	(0.3)
γ-CD																
O3–H···O2′	160.7	(3.8)			161.2	(1.8)					159.9	(1.1)	161.3	(3.0)		
O2–H···O3′			149.7	(0.5)			150.1	(2.0)	150.7	(0.3)					152.6	(4.3)
O6–H···O6′	161.4	(0.7)	161.3	(2.7)	162.2	(3.5)	161.2	(1.1)								
O6–H···O5′									149.2	(1.0)	151.3	(2.5)				
O6–H···O5													102.9	(1.5)	103.3	(1.4)

these interactions, and the low angles of interaction, mean that they are likely to be weaker than the hydroxyl–hydroxyl interactions. Additionally, for C-type conformers, the distances and angles of the O6–H···O5 interactions imply that they may be of a dispersive nature.

Based on these results, it can be stated that the B- and C-type conformers are likely to be more flexible and to interact more strongly with the surrounding water molecules when in solution, in agreement with results of the thermodynamic and NMR analyses. However, geometrical parameters do not provide enough information to allow us to classify and sort these interactions. Therefore, to classify the interactions, a QTAIM analysis was performed. Bond critical points were calculated for all possible interactions in all 24 conformers. Table 7 presents the results of this analysis for conformers B3 and C1, as they presented the most accurate NMR results. Tables S11–S16 of the ESM show the results of QTAIM analysis for all the conformers.

According to Nakanishi's classification of interactions [69, 70], based on the ρ_c values, all the hydrogen interactions are typical hydrogen bonds. Since $\nabla^2\rho_c > 0$ for all the interactions, they can be classified as closed shell with a certain degree of

Table 7 Mean values (and standard deviations) of the electron density (ρ_c), the Laplacian of the electron density ($\nabla^2\rho_c$), the total energy density (H_c), and the ellipticity of the electron density (ε) at BCPs for hydrogen interactions in the conformers, as calculated at the SMD/M06-2X-D3/6-31G(d,p) level of theory with water as the solvent using QTAIM [a]

Interaction	$\rho_c \times 10^2$				$\nabla^2\rho_c \times 10^2$				$H_c \times 10^3$				$\varepsilon \times 10^2$			
	B3		C1		B3		C1		B3		C1		B3		C1	
α-CD																
O3–H···O2′	1.69	(0.03)	2.34	(0.02)	4.87	(0.09)	6.92	(0.10)	−0.78	(0.02)	−0.83	(0.05)	4.16	(0.17)	6.05	(0.09)
O6–H···O5′	2.16	(0.09)	–	–	6.65	(0.26)	–	–	−0.90	(0.05)	–	–	8.39	(0.39)	–	–
β-CD																
O3–H···O2′	1.95	(0.03)	2.42	(0.07)	5.72	(0.12)	7.32	(0.23)	−0.84	(0.01)	−0.72	(0.05)	5.75	(0.18)	6.95	(0.14)
O6–H···O5′	2.26	(0.08)	–	–	6.95	(0.22)	–	–	−0.92	(0.03)	–	–	8.09	(0.36)	–	–
γ-CD																
O3–H···O2′	2.06	(0.01)	2.45	(0.15)	6.15	(0.05)	7.47	(0.41)	−0.80	(0.05)	−0.66	(0.14)	6.63	(0.16)	7.10	(0.13)
O6–H···O5′	2.37	(0.11)	–	–	7.31	(0.31)	–	–	−0.90	(0.02)	–	–	7.77	(0.73)	–	–

[a] All values are given in atomic units

covalency (given that $H_c < 0$). As $\varepsilon \approx 0$ for these interactions, the electron density distributions appear to be cylindrical, implying directional interactions (as opposed to other nondirectional weak interactions such as van der Waals) [77].

Noting the ρ_c and $\nabla^2\rho_c$ values for the interactions involving secondary hydroxyls (O3–H···O2′), it can be argued that the C1 conformers have the highest values of ρ_c, suggesting that they exhibit the strongest interactions. However, the values of $\nabla^2\rho_c$ suggest that the B3 conformers have the strongest charge-transfer character, although differences among the conformers are rather small. It is the opinion of the authors that these small differences do not favor one conformer over the other in the stability or strength of their interactions. In terms of interactions involving the primary hydroxyl groups, only B3 presents a hydroxyl–ether interaction (O6–H···O5′), as no BCP involving this group was found for the C1 conformers, meaning that the primary hydroxyls are free to interact with the surrounding medium. The hydroxyl–ether interactions observed in B3 are relatively stable compared to the O3–H···O2′ interactions in both B3 and C1. However, the groups involved in the O6–H···O5′ interactions are still able to interact with their surroundings due to the nonlinear geometries of the interactions.

Summary

We have presented the results of the computational modeling of several symmetrical conformers of α-, β-, and γ-cyclodextrin. The method SMD/M06-2X/6-31G(d,p) was found to accurately describe the conformers in terms of their bond distances and angles, as shown by a comparison with experimental X-ray diffraction geometries. The calculations showed that all of the studied conformers are stable in the gas phase and in aqueous solution and may coexist in a real system. Theoretical thermodynamical and NMR analyses indicated that the B and C conformers are the most populated in aqueous solution, while the A conformers dominate in the gas phase. The use of theoretically calculated dipole moments remains a questionable criterion for deciding which of the conformers most accurately describes a particular CD in solution. The main noncovalent interactions present in these conformers were found to be typical hydrogen bonds between the hydroxyl groups of the cyclodextrins. For the B-type conformers, hydroxyl–ether hydrogen bonds with O6–H groups were identified, while the C-type conformers do not show interactions involving O6–H. The results of this work will be used to construct a cyclodextrin model that can be applied when studying host–guest complexes involving cyclodextrins.

Acknowledgements Computational calculations were performed using Wahoo, the cluster of the Centre Commun de Calcul Intensif of the Université des Antilles, Guadeloupe, France. Several calculations were run in the computer clusters Brutus and Euler at ETH, Zürich, Switzerland. The informatics service at InSTEC, Havana, Cuba is gratefully acknowledged for allowing communications with calculation centers overseas. The authors also wish to express their gratitude for the financial support provided by the project TATARCOP-InSTEC, Havana, and to the Cooperation Service of the French Embassy in Havana, Cuba.

References

1. Szejtli J (1998) Introduction and general overview of cyclodextrin chemistry. Chem Rev 98(5):1743–1754. https://doi.org/10.1021/cr970022c
2. Tonkova A (1998) Bacterial cyclodextrin glucanotransferase. Enzym Microb Technol 22(8):678–686. https://doi.org/10.1016/S0141-0229(97)00263-9
3. Biwer A, Antranikian G, Heinzle E (2002) Enzymatic production of cyclodextrins. Appl Microbiol Biotechnol 59(6):609–617. https://doi.org/10.1007/s00253-002-1057-x
4. Del Valle EMM (2004) Cyclodextrins and their uses: a review. Process Biochem 39(9):1033–1046. https://doi.org/10.1016/S0032-9592(03)00258-9
5. Manor PC, Saenger W (1974) Topography of cyclodextrin inclusion complexes. III. Crystal and molecular structure of cyclohexaamylose hexahydrate, the water dimer inclusion complex. J Am Chem Soc 96(11):3630–3639
6. Steiner T, Koellner G (1994) Crystalline β-cyclodextrin hydrate at various humidities: fast, continuous, and reversible dehydration studied by X-ray diffraction. J Am Chem Soc 116(12):5122–5128
7. Harata K (1987) The structure of the cyclodextrin complex. XX. Crystal structure of uncomplexed hydrated γ-cyclodextrin. Bull Chem Soc Jap 60:2763–2767
8. Frömming K-H, Szejtli J (1994) Cyclodextrins in pharmacy, vol 5, 1st edn. Springer, Dordrecht
9. Loftsson T, Brewster ME (1996) Pharmaceutical applications of cyclodextrins. 1. Drug solubilization and stabilization. J Pharm Sci 85(10):1017–1025
10. Szejtli J (2004) Past, present and futute of cyclodextrin research. Pure Appl Chem 76(10):1825–1845
11. Steed J, Atwood J (2009) Supramolecular chemistry, 2nd edn. Wiley, Chichester
12. Connors KA (1997) The stability of cyclodextrin complexes in solution. Chem Rev 97(5):1325–1358
13. Rekharsky MV, Inoue Y (1998) Complexation thermodynamics of cyclodextrins. Chem Rev 98(5):1875–1918
14. Loftsson T, Duchêne D (2007) Cyclodextrins and their pharmaceutical applications. Int J Pharm 329(1):1–11
15. Juvancz Z, Kendrovics RB, Iványi R, Szente L (2008) The role of cyclodextrins in chiral capillary electrophoresis. Electrophoresis 29(8):1701–1712. https://doi.org/10.1002/elps.200700657
16. Dodziuk H (2006) Cyclodextrins and their complexes: chemistry, analytical methods, applications. Wiley-VCH, Weinheim
17. Szejtli J (ed)(1981) Advances in inclusion science. Proceedings of the First International Symposium on Cyclodextrins. Springer, Dordrecht
18. Szejtli J, Osa T (eds)(1996) Cyclodextrins, vol 3. Comprehensive supramolecular chemistry. Pergamon/Elsevier, Oxford
19. Hedges AR (1998) Industrial applications of cyclodextrins. Chem Rev 98(5):2035–2044. https://doi.org/10.1021/cr970014w
20. Uekama K (2002) Recent aspects of pharmaceutical application of cyclodextrins. J Incl Phenom Macrocycl Chem 44(1–4):3–7. https://doi.org/10.1023/A:1023007032444

21. Bilensoy E (ed)(2011) Cyclodextrins in pharmaceutics, cosmetics, and biomedicine: current and future industrial applications. Wiley, Hoboken
22. Stella VJ, Rajewski RA (1997) Cyclodextrins: their future in drug formulation and delivery. Pharm Res 14(5):556–567
23. Szente L, Szemán J (2013) Cyclodextrins in analytical chemistry: host-guest type molecular recognition. Anal Chem 85(17):8024–8030
24. Shao D, Sheng G, Chen C, Wang X, Nagatsu M (2010) Removal of polychlorinated biphenyls from aqueous solutions using β-cyclodextrin grafted multiwalled carbon nanotubes. Chemosphere 79(7):679–685
25. Fakayode SO, Lowry M, Fletcher KA, Huang X, Powe AM, Warner IM (2007) Cyclodextrins host-guest chemistry in analytical and environmental chemistry. Curr Anal Chem 3(3):171–181
26. Gruiz K, Molnár M, Fenyvesi E, Hajdu C, Atkári Á, Barkács K (2011) Cyclodextrins in innovative engineering tools for risk-based environmental management. J Incl Phenom Macrocycl Chem 70(3–4):299–306
27. Simó C, Barbas C, Cifuentes A (2003) Chiral electromigration methods in food analysis. Electrophoresis 24(15):2431–2441. https://doi.org/10.1002/elps.200305442
28. Cabral Marques HM (2010) A review on cyclodextrin encapsulation of essential oils and volatiles. Flavour Fragr J 25(5):313–326. https://doi.org/10.1002/ffj.2019
29. Schneiderman E, Stalcup AM (2000) Cyclodextrins: a versatile tool in separation science. J Chromatogr B 745(1):83–102. https://doi.org/10.1016/S0378-4347(00)00057-8
30. Li S, Purdy WC (1992) Cyclodextrins and their applications in analytical chemistry. Chem Rev 92(6):1457–1470
31. Mosinger J, Tománková V, Němcová I, Zýka J (2001) Cyclodextrins in analytical chemistry. Anal Lett 34(12):1979–2004
32. Muñoz de la Peña A, Mahedero M, Sánchez AB (2000) Room temperature phosphorescence in cyclodextrins. Analytical applications. Analysis 28(8):670–678
33. Lipkowitz KB (1998) Applications of computational chemistry to the study of cyclodextrins. Chem Rev 98(5):1829–1874. https://doi.org/10.1021/cr9700179
34. Maclennan JM, Stezowski JJ (1980) The crystal structure of uncomplexed-hydrated cyclooctaamylose. Biochem Biophys Res Commun 92(3):926–932
35. Lindner K, Saenger W (1982) Crystal and molecular structure of cyclohepta-amylose dodecahydrate. Carbohydr Res 99:103–115
36. Endo T, Nagase H, Ueda H, Kobayashi S, Nagai T (1997) Isolation, purification, and characterization of cyclomaltodecaose (ε-Cyclodextrin), cyclomaltoundecaose (ζ-cyclodextrin) and cyclomaltotridecaose (θ-cyclodextrin). Chem Pharm Bull 45(3):532–536. https://doi.org/10.1248/cpb.45.532
37. Momany FA, Willett JL (2000) Computational studies on carbohydrates: solvation studies on maltose and cyclomaltooligosaccharides (cyclodextrins) using a DFT/ab initio-derived empirical force field, AMB99C. Carbohydr Res 326(3):210–226. https://doi.org/10.1016/S0008-6215(00)00043-4
38. Mixcoha E, Campos-Terán J, Piñeiro Á (2014) Surface adsorption and bulk aggregation of cyclodextrins by computational molecular dynamics simulations as a function of temperature: α-CD vs β-CD. J Phys Chem B 118(25):6999–7011. https://doi.org/10.1021/jp412533b
39. Koehler J, Saenger W, Van Gunsteren W (1988) On the occurrence of three-center hydrogen bonds in cyclodextrins in crystalline form and in aqueous solution: comparison of neutron diffraction and molecular dynamics results. J Biomol Struct Dyn 6(1):181–198
40. Koehler J, Saenger W, Van Gunsteren W (1988) Conformational differences between α-cyclodextrin in aqueous solution and in crystalline form: a molecular dynamics study. J Mol Biol 203(1):241–250
41. Elbashir AA, Suliman FO (2011) Computational modeling of capillary electrophoretic behavior of primary amines using dual system of 18-crown-6 and β-cyclodextrin. J Chromatogr A 1218(31):5344–5351
42. Nascimento Jr CS, Dos Santos HF, De Almeida WB (2004) Theoretical study of the formation of the α-cyclodextrin hexahydrate. Chem Phys Lett 397(4):422–428
43. Anconi CPA, Nascimento CS, Fedoce-Lopes J, Dos Santos HF, De Almeida WB (2007) Ab initio calculations on low-energy conformers of α-cyclodextrin. J Phys Chem A 111(48):12127–12135. https://doi.org/10.1021/jp0762424
44. Snor W, Liedl E, Weiss-Greiler P, Karpfen A, Viernstein H, Wolschann P (2007) On the structure of anhydrous β-cyclodextrin. Chem Phys Lett 441(1):159–162
45. Pinjari RV, Joshi KA, Gejji SP (2006) Molecular electrostatic potentials and hydrogen bonding in α-, β-, and γ-cyclodextrins. J Phys Chem A 110(48):13073–13080
46. Pinjari RV, Joshi KA, Gejji SP (2007) Theoretical studies on hydrogen bonding, NMR chemical shifts and electron density topography in α, β and γ-cyclodextrin conformers. J Phys Chem A 111(51):13583–13589. https://doi.org/10.1021/jp074539w
47. Karpfen A, Liedl E, Snor W, Weiss-Greiler P, Viernstein H, Wolschann P (2007) Homodromic hydrogen bonds in low-energy conformations of single molecule cyclodextrins. J Incl Phenom Macrocycl Chem 57(1–4):35–38
48. Jiménez V, Alderete JB (2008) Hartree−Fock and density functional theory study of α-cyclodextrin conformers. J Phys Chem A 112(4):678–685. https://doi.org/10.1021/jp073011o
49. Deshmukh MM, Bartolotti LJ, Gadre SR (2011) Intramolecular hydrogen bond energy and cooperative interactions in α-, β-, and γ-cyclodextrin conformers. J Comput Chem 32(14):2996–3004. https://doi.org/10.1002/jcc.21881
50. Stachowicz A, Styrcz A, Korchowiec J, Modaressi A, Rogalski M (2011) DFT studies of cation binding by β-cyclodextrin. Theor Chem Acc 130(4):939–953
51. Jaiyong P, Bryce RA (2017) Approximate quantum chemical methods for modelling carbohydrate conformation and aromatic interactions: β-cyclodextrin and its adsorption on a single-layer graphene sheet. Phys Chem Chem Phys 19:15346–15355
52. Zhao Y, Truhlar DG (2008) The M06 suite of density functionals for main group thermochemistry, thermochemical kinetics, noncovalent interactions, excited states, and transition elements: two new functionals and systematic testing of four M06-class functionals and 12 other functionals. Theor Chem Acc 120(1):215–241
53. Stewart JJP (2007) Optimization of parameters for semiempirical methods. V: Modification of NDDO approximations and application to 70 elements. J Mol Model 13:1173–1213. https://doi.org/10.1007/s00894-007-0233-4
54. Grimme S, Antony J, Ehrlich S, Krieg H (2010) A consistent and accurate ab initio parametrization of density functional dispersion correction (DFT-D) for the 94 elements H–Pu. J Chem Phys 132(15):154104
55. Řezáč J, Hobza P (2011) Advanced corrections of hydrogen bonding and dispersion for semiempirical quantum mechanical methods. J Chem Theory Comput 8(1):141–151
56. Stewart JJP (2016) MOPAC2016 v16.125W. Stewart Computational Chemistry, Colorado Springs
57. Grimme S, Ehrlich S, Goerigk L (2011) Effect of the damping function in dispersion corrected density functional theory. J Comput Chem 32(7):1456–1465. https://doi.org/10.1002/jcc.21759
58. Marenich AV, Cramer CJ, Truhlar DG (2009) Universal solvation model based on solute electron density and on a continuum model of the solvent defined by the bulk dielectric constant and atomic surface tensions. J Phys Chem B 113(18):6378–6396

59. Frisch MJ, Trucks GW, Schlegel HB, Scuseria GE, Robb MA, Cheeseman JR, Scalmani G, Barone V, Mennucci B, Petersson GA, Nakatsuji H, Caricato M, Li X, Hratchian HP, Izmaylov AF, Bloino J, Zheng G, Sonnenberg JL, Hada M, Ehara M, Toyota K, Fukuda R, Hasegawa J, Ishida M, Nakajima T, Honda Y, Kitao O, Nakai H, Vreven T, Montgomery Jr JA, Peralta JE, Ogliaro F, Bearpark M, Heyd JJ, Brothers E, Kudin KN, Staroverov VN, Kobayashi R, Normand J, Raghavachari K, Rendell A, Burant JC, Iyengar SS, Tomasi J, Cossi M, Rega N, Millam JM, Klene M, Knox JE, Cross JB, Bakken V, Adamo C, Jaramillo J, Gomperts R, Stratmann RE, Yazyev O, Austin AJ, Cammi R, Pomelli C, Ochterski JW, Martin RL, Morokuma K, Zakrzewski VG, Voth GA, Salvador P, Dannenberg JJ, Dapprich S, Daniels AD, Farkas O, Foresman JB, Ortiz JV, Cioslowski J, Fox DJ (2013) Gaussian 09, revision E.01. Gaussian, Inc., Wallingford
60. London F (1937) Théorie quantique des courants interatomiques dans les combinaisons aromatiques. J Phys Radium 8(10):397–409
61. Young DC (2001) Computational chemistry: a practical guide for applying techniques to real-world problems. Wiley, New York
62. Rablen PR, Pearlman SA, Finkbiner J (1999) A comparison of density functional methods for the estimation of proton chemical shifts with chemical accuracy. J Phys Chem A 103(36):7357–7363
63. Sebag AB, Forsyth DA, Plante MA (2001) Conformation and configuration of tertiary amines via GIAO-derived ^{13}C NMR chemical shifts and a multiple independent variable regression analysis. J Org Chem 66(24):7967–7973
64. Brown I (1976) On the geometry of O–H···O hydrogen bonds. Acta Crystallogr Sect A 32(1):24–31
65. Ferraris G, Ivaldi G (1988) Bond valence vs bond length in O···O hydrogen bonds. Acta Crystallogr Sect B 44(4):341–344
66. Smallwood CJ, McAllister MA (1997) Characterization of low-barrier hydrogen bonds. 7. Relationship between strength and geometry of short-strong hydrogen bonds. The formic acid− formate anion model system. An ab initio and DFT investigation. J Am Chem Soc 119(46):11277–11281
67. Grabowski SJ (2004) Hydrogen bonding strength—measures based on geometric and topological parameters. J Phys Org Chem 17(1): 18–31
68. Bader RFW (1994) Atoms in molecules: a quantum theory, vol 22, 1st edn. Clarendon, Oxford
69. Nakanishi W, Hayashi S, Narahara K (2008) Atoms-in-molecules dual parameter analysis of weak to strong interactions: behaviors of electronic energy densities versus Laplacian of electron densities at bond critical points. J Phys Chem A 112(51):13593–13599. https://doi.org/10.1021/jp8054763
70. Nakanishi W, Hayashi S, Narahara K (2009) Polar coordinate representation of $H_b(r_c)$ versus $(\hbar^2/8m)\nabla^2\rho_b(r_c)$ at BCP in AIM analysis: classification and evaluation of weak to strong interactions. J Phys Chem 113:10050–10057. https://doi.org/10.1021/jp903622a
71. Kitagawa M, Hoshi H, Sakurai M, Inoue Y, Chûjô R (1987) The large dipole moment of cyclomaltohexaose and its role in determining the guest orientation in inclusion complexes. Carbohydr Res 163(1):c1–c3
72. Sakurai M, Kitagawa M, Hoshi H, Inoue Y, Chûjô R (1990) A molecular orbital study of cyclodextrin (cyclomaltooligosaccharide) inclusion complexes. III: Dipole moments of cyclodextrins in various types of inclusion complex. Carbohydr Res 198(2):181–191
73. Rajendiran N, Sankaranarayanan R (2014) Azo dye/cyclodextrin: new findings of identical nanorods through 2:2 inclusion complexes. Carbohydr Polym 106:422–431
74. Schneider H-J, Hacket F, Volker R, Ikeda H (1998) NMR studies of cyclodextrins and cyclodextrin complexes. Chem Rev 98:1755–1785
75. Giesen DJ, Zumbulyadis N (2002) A hybrid quantum mechanical and empirical model for the prediction of isotropic ^{13}C shielding constants of organic molecules. Phys Chem Chem Phys 4(22): 5498–5507
76. Saenger W, Steiner T (1998) Cyclodextrin inclusion complexes: host–guest interactions and hydrogen-bonding networks. Acta Crystallogr Sect A 54(6):798–805
77. Gamboa-Carballo JJ, Melchor-Rodríguez K, Hernández-Valdés D, Enriquez-Victorero C, Montero-Alejo AL, Gaspard S, Jáuregui-Haza UJ (2016) Theoretical study of chlordecone and surface groups interaction in an activated carbon model under acidic and neutral conditions. J Mol Graph Model 65:83–93. https://doi.org/10.1016/j.jmgm.2016.02.008